

## **REMARKS/ARGUMENTS**

### **STATUS OF THE CLAIMS**

Claims 104-111, 113-140, and 286 are pending with entry of this amendment, claims 1-103, 112, 141-193, and 194-285 having been cancelled previously. Claims 104 and 286 are amended herein. These amendments introduce no new matter and support is replete throughout the specification. These amendments are made without prejudice to renewal of the claims in their original form and are not to be construed as abandonment or dedication of the previously claimed subject matter or agreement with any objection or rejection of record.

Claim 104 has been amended to specify that the photoactive layer is free of conductive polymer, removing the term "substantially." Claim 286 has been amended to specify that the photoactive layer comprises a first population of nanostructures and a conductive polymer whose charge carrying properties have been altered during fabrication of the device by controlled partial oxidation of the polymer, removing the phrase "and/or a small molecule."

Applicants submit that no new matter has been added to the application by way of the above claim amendments. Accordingly, entry of the Amendment is respectfully requested.

The action of April 29, 2008 included: discussion of priority, claim rejections for alleged indefiniteness, claim rejections for alleged anticipation, and claim rejections for alleged obviousness. Applicants traverse all rejections and objections, to the extent that they may be applied to the amended claims, for the reasons noted herein.

### **THE INFORMATION DISCLOSURE STATEMENTS**

Applicants note with appreciation the Examiner's thorough consideration of the references cited in the Information Disclosure Statement (Form 1449) submitted on January 23, 2008.

Applicants note they have previously submitted two Information Disclosure Statements (Forms 1449), dated July 14, 2004 and July 23, 2004. Applicants request that the Examiner indicate consideration of the citations by initialing the 1449 documents and providing a copy to Applicants.

PRIORITY (ACTION ITEM 1)

Applicants note that the instant application as filed correctly claimed priority to U.S. Patent Application No. 10/656,802, which in turn claims priority to U.S. Provisional Patent Applications 60/452,038, 60/421,353, and 60/408,722.

In response to the Action's allegation that "Application Nos. 10/656802, 60/452038, 60/421353 do not contain subject matter such as 'the photoactive layer is substantially free of conductive polymer,'" Applicants note that photoactive layers substantially free of any conductive polymer are described, e.g., in priority application 10/656,802 at paragraph 27. Further, the desirability of eliminating conductive polymer from the active layer is described, e.g., in priority applications 60/452,038 at paragraph at paragraphs 29 and 46 and 60/421353 at paragraphs 28 and 44.

THE CLAIMS, AS AMENDED, ARE DEFINITE (ACTION ITEM 3)

Claim 104 was rejected under 35 USC §112, second paragraph, for alleged indefiniteness with respect to use of the term "substantially." Applicants have amended claim 104 to remove this term, rendering the rejection moot. Accordingly, Applicants request the rejection be withdrawn.

Claim 104 was also rejected for alleged indefiniteness with respect to use of the phrase "discrete nanostructures." The Action alleges that it is unclear what "discrete nanostructures" refers to. Applicants note that the term "discrete" is used in its ordinary meaning of "constituting a separate entity : individually distinct" (Merriam-Webster's Online Dictionary). The term "discrete nanostructures" thus refers to separate, individually distinct nanostructures (as opposed, for example, to a network of interconnected tubules that are not individually distinct). Applicants respectfully request the rejection be reconsidered and withdrawn.

Claim 111 was rejected for alleged indefiniteness with respect to use of the phrase "the small molecule dispersed in a non-conductive polymer." The Action alleges that it is unclear how a small molecule, or a single molecule, can be dispersed in a polymer. Applicants directs the Examiner's attention to the definition of "a" at paragraph 106, which reads "As used in this specification and the appended claims, the singular forms 'a,' 'an' and 'the' include plural referents unless the context clearly dictates otherwise. Thus, for

example, reference to 'a nanostructure' includes a plurality of nanostructures, and the like." The term "small molecule" thus includes a plurality of copies of the small molecule, which, as is clear from the context, can be dispersed in a polymer. Applicants respectfully request the rejection be reconsidered and withdrawn.

THE CLAIMS ARE FREE OF SAGER (ACTION ITEM 4)

Claims 104-113, 115-119, and 121-129 were rejected for alleged anticipation under 35 USC 102(e) by Sager et al. (USPN 6,946,597). To the extent that the rejections are applied to the amended claims, Applicants respectfully traverse.

In order for a reference to anticipate an invention, the reference must teach each and every element of the claimed invention. Sager, however, fails to teach at least a photoactive layer comprising discrete nanostructures and substantially free of conductive polymer, as detailed below.

The Action equates the first charge transfer material of Sager to nanostructures of the instant invention. However, Applicants note that the first charge transfer material of Sager is used to coat the pores of a mesoporous material (see, e.g., column 9 lines 3-4) and does not form discrete nanostructures corresponding to those of the instant invention. See, e.g., Figures 1A, 1C, and 1D of Sager, which clearly demonstrate that first charge transfer material 107 does not correspond to individual, discrete nanostructures such as those specified in claim 104. (See also Sager Figure 3.) Sager thus fails to teach discrete nanostructures.

The Action alleges that "Sager et al. teaches the second charge transfer layer including a non-conducting polymer such as polyfluorenes and polyfluorene-based copolymers," and further alleges that "the photoactive layer is substantially free of conductive polymer since polyfluorene is not conductive" (Action at page 4). However, Applicants note that polyfluorene is, in fact, a conductive polymer. See, for example, the attached reference describing growth of polyfluorene (Sharma and Park (2004) "Electrochemistry of conductive polymers: XXIX. Polyfluorene growth in dichloromethane and acetonitrile: A comparative study" J Electrochem Soc 151(2):E61-E68), which clearly states that polyfluorene is a conducting polymer (e.g., at the second sentence of column 1).

See also Applicants' disclosure at paragraph 129. Sager thus fails to teach a photoactive layer free of conductive polymer.

Additional points of distinction are present in the dependent claims, but because independent claim 104 is not anticipated, it is not necessary to address each additional point.

Because Sager does not teach at least a photoactive layer comprising discrete nanostructures and substantially free of conductive polymer meeting the limitations of claim 104, Applicants respectfully request the rejections be withdrawn.

THE CLAIMS ARE NOT OBVIOUS (ACTION ITEMS 5-10)

Item 5

Claims 114 and 120 were rejected for alleged obviousness under 35 USC 103(a) over Sager in view of Alivisatos et al (U.S. patent publication 2003/0226498). Applicants respectfully traverse these rejections.

As recently reaffirmed by the Supreme Court in KSR International Co. v. Teleflex, Inc. (550 U.S. \_\_\_, 82 USPQ2d 1385 (2007)), the appropriate standard for analyzing questions of obviousness is that

“the scope and content of the prior art are determined, differences between the prior art and the claims at issue are analyzed and the level of ordinary skill in the pertinent art is resolved. Against this background the obviousness or non-obviousness of the subject matter is determined. Such secondary considerations as commercial success, long felt but unresolved needs, failure of others, etc. might be utilized to give light to the circumstances surrounding the origin of the subject matter to be patented.

*Id.* quoting Graham v. John Deere of Kansas City 383 U.S. 1, 17-18.

This Graham v. John Deere standard has long been interpreted by the Office to mean that three requirements must be met for a *prima facie* case of obviousness. First, the prior art reference(s) must teach or suggest all of the limitations of the claims (M.P.E.P. § 2143.03). Second, there must be a motivation to modify the reference or combine the teachings to produce the claimed invention (M.P.E.P. § 2143.01). Third, a reasonable expectation of success is required (M.P.E.P. § 2143.02).

A recent memorandum (dated May 3, 2007) from the Deputy Commissioner to the Technology Center Directors regarding the KSR/Graham standard reiterates that, while “The

Court rejected a rigid application of the ‘teaching, suggestion, or motivation’ (TSM) test,” it “did not totally reject the use of ‘teaching, suggestion, or motivation’ as a factor in the obviousness analysis.” The memo concludes that “in formulating a rejection under 35 U.S.C. § 103(a) based upon a combination of prior art elements, it remains necessary to identify the reason why a person of ordinary skill in the art would have combined the prior art elements in the manner claimed” (emphasis added). Similarly, guidelines for examination recently published in the Federal Register (vol. 72 no. 195 p. 57526-57535) also highlight the need for “clear articulation of the reason(s) why the claimed invention would have been obvious” (p. 57528).

Application of the KSR/Graham standard in the present case indicates that the claims at issue are not obvious.

First, the combination of Sager and Alivisatos fails to teach all the limitations of the claims. As described above with respect to claim 104, Sager fails to teach at least a photoactive layer that comprises discrete nanostructures and that is substantially free of conductive polymer. Merely adding nanowires or branched nanocrystals from Alivisatos thus still fails to teach all the limitations of the claims.

In addition, motivation to combine the teachings of the references is lacking and there is no reasonable expectation of success, e.g., because the suggested combination does not result in the present invention

Applicants respectfully request that the rejections be reconsidered and withdrawn.

#### Item 6

Claims 130-133 were rejected for alleged obviousness under 35 USC 103(a) over Sager. Applicants respectfully traverse these rejections.

The suggested modification of Sager does not meet the requirements for a *prima facie* case of obviousness. First, the suggested modification does not teach all the limitations of the claims. As described above, Sager fails to teach all the limitations of claim 104 from which claims 130-133 depend. As noted in the Action, Sager also fails to teach the device in a non-planar or convex architecture or the electrode and photoactive layers oriented in a coiled or reciprocating stacked architecture. The Action alleges that because the device of Sager is flexible it is obvious to configure it in a non-planar, convex, coiled, or reciprocating

stacked architecture. Applicants note, however, that merely because the device of Sager is, *arguendo*, potentially capable of assuming such architectures does not mean it is obvious to form it into such configurations. No reason for doing so based on the art rather than on Applicants' disclosure has been identified. Since no rationale for modifying the teachings of Sager has been established, the argument presented in the Action that the reference be modified involves an improper hindsight reconstruction of the invention. Moreover, there is no reasonable expectation of success since the suggested combination does not result in the present invention. Accordingly, Applicants respectfully request that the rejections be withdrawn.

Item 7

Claims 134-136 were rejected for alleged obviousness under 35 USC 103(a) over Sager in view of Simmons (USPN 5,720,827. Applicants respectfully traverse.

The combination of Sager and Simmons does not meet the requirements for a *prima facie* case of obviousness. First, the suggested combination does not teach all the limitations of the claims. As described above, Sager fails to teach all the limitations of claim 104 from which claims 134-136 depend; e.g., Sager fails to teach at least a photoactive layer that is substantially free of conductive polymer and that includes discrete nanostructures. Merely adding different nanocrystal subpopulations from Simmons thus still fails to teach all the limitations of the claims.

In addition, motivation to combine the teachings of the references is lacking and there is no reasonable expectation of success, e.g., because the suggested combination does not result in the present invention

Applicants respectfully request that the rejections be reconsidered and withdrawn.

Item 8

Claims 137-138 were rejected for alleged obviousness under 35 USC 103(a) over Sager in view of Salafsky (US 6,239,355). Applicants respectfully traverse.

The combination of Sager and Salafsky does not meet the requirements for a *prima facie* case of obviousness. First, the suggested combination does not teach all the limitations of the claims. As described above, Sager fails to teach all the limitations of claim 104 from which claims 137-138 depend. Merely adding a second photoactive layer or a second

photoactive layer and third and fourth electrodes from Salafsky thus still fails to teach all the limitations of the claims.

In addition, motivation to combine the teachings of the references is lacking and there is no reasonable expectation of success, e.g., because the suggested combination does not result in the present invention

Applicants respectfully request that the rejections be reconsidered and withdrawn.

Item 9

Claims 139-140 were rejected for alleged obviousness under 35 USC 103(a) over Sager in view of Ono (U.S. patent publication 2003/0013008). Applicants respectfully traverse.

The combination of Sager and Ono does not meet the requirements for a *prima facie* case of obviousness.

First, the suggested combination does not teach all the limitations of the claims. With respect to claims 139-140, as described above Sager fails to teach all the limitations of claim 104 from which claims 139-140 depend. Sager (and thus the combination of Sager and Ono) fails to teach at least a photoactive layer that is substantially free of conductive polymer and that includes discrete nanostructures.

In addition, with respect to claim 140, the combination of Sager and Ono also fails to teach a first recombination material disposed between and in at least partial electrical contact with the first and second photoactive layers. Although the Action equates the third electrode of Ono to a recombination material, as detailed in Applicants' previously filed response the electrode of Ono transports charge carriers, in contrast to a recombination material of the instant invention within which holes and electrons recombine rather than being transported through the material. Ono thus fails to teach a recombination material meeting the limitations of claim 140.

In addition, motivation to combine the teachings of the references is lacking and there is no reasonable expectation of success, e.g., because the suggested combination does not result in the present invention

Applicants respectfully request that the rejections be reconsidered and withdrawn.

Item 10

Claim 286 was rejected for alleged obviousness under 35 USC 103(a) over Sager in view of Ono. To the extent that the rejections are applied to the amended claim, Applicants respectfully traverse.

As noted above, claim 286 has been amended to specify that the photoactive layer comprises a first population of nanostructures and a conductive polymer whose charge carrying properties have been altered during fabrication of the device by controlled partial oxidation of the polymer, removing the phrase “and/or a small molecule” and rendering the rejection moot.

DOUBLE PATENTING (ACTION ITEMS 11-12)

The claims were rejected for alleged nonstatutory obviousness-type double patenting over claims 1-83 of U.S. Patent 6,878,871 in view of Sager and over claims 1-24 of U.S. Patent 7,087,832 in view of Sager.

As noted above, Sager fails to teach at least a photoactive layer free of conductive polymer. Applicants therefore respectfully request the rejections be withdrawn.

**CONCLUSION**

In view of the foregoing, Applicant(s) believe(s) all claims now pending in this application are in condition for allowance. The issuance of a formal Notice of Allowance at an early date is respectfully requested.

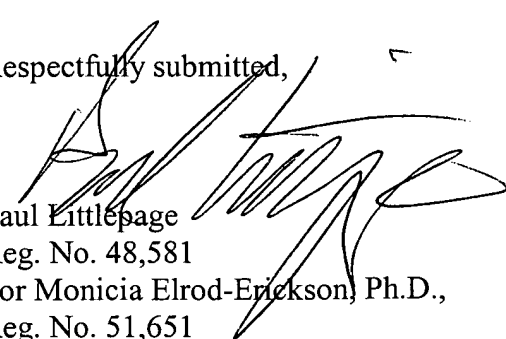
If the claims are deemed not to be in condition for allowance after consideration of this Response, a telephone interview with the Examiner is hereby requested. Please telephone Monica Elrod-Erickson at (510) 337-7871 to schedule an interview.



Appl. No. 10/778,009  
Amdt. Dated 6/30/2008  
Reply to Office action of April 29, 2008

QUINE INTELLECTUAL PROPERTY LAW GROUP  
P.O. BOX 458, Alameda, CA 94501  
Tel: 510 337-7871  
Fax: 510 337-7877  
PTO Customer No.: **22798**  
Deposit Account No.: **50-0893**

Respectfully submitted,



Paul Littlepage  
Reg. No. 48,581  
For Monica Elrod-Erickson, Ph.D.,  
Reg. No. 51,651

Attachments:

- 1) A transmittal sheet;
- 2) Sharma and Park (2004) "Electrochemistry of conductive polymers:  
XXIX. Polyfluorene growth in dichloromethane and acetonitrile: A  
comparative study" J Electrochem Soc 151(2):E61-E68; and
- 3) A receipt indication postcard.



## Electrochemistry of Conductive Polymers

### XXIX. Polyfluorene Growth in Dichloromethane and Acetonitrile: A Comparative Study

H. S. Sharma<sup>a</sup> and Su-Moon Park<sup>\*z</sup>

Department of Chemistry and Center for Integrated Molecular Systems, Pohang University of Science and Technology, Pohang 790-784, Korea

A comparative study on polyfluorene (PFI) growth has been carried out in dichloromethane ( $\text{CH}_2\text{Cl}_2$ ) and acetonitrile ( $\text{CH}_3\text{CN}$ ) solutions employing cyclic voltammetry, kinetic measurements, electrochemical quartz crystal microbalance (EQCM) and *in situ* spectroelectrochemical techniques. The results indicate that fluorene is polymerized more effectively in  $\text{CH}_3\text{CN}$  than in  $\text{CH}_2\text{Cl}_2$ , and the PFI films prepared in  $\text{CH}_3\text{CN}$  generally have better physicochemical characteristics than those in  $\text{CH}_2\text{Cl}_2$ . The polymerization reaction rates fluctuate due to the passivation/depassivation processes taking place in  $\text{CH}_2\text{Cl}_2$ , while they decrease steadily with increasing potential cycle number in  $\text{CH}_3\text{CN}$ . EQCM studies show that the current efficiencies are about 100% in  $\text{CH}_3\text{CN}$ , while they average about 25% in  $\text{CH}_2\text{Cl}_2$ . Spectroelectrochemical studies show that monomers are quickly polymerized to make long-chain oligomers in  $\text{CH}_3\text{CN}$ , while the chain lengths are generally shorter for polymers prepared in  $\text{CH}_2\text{Cl}_2$ . These differences are attributed to the differences in solvent characteristics such as their dielectric constants, leading to a different solubility of oligomers and different ion stabilization.

© 2004 The Electrochemical Society. [DOI: 10.1149/1.1639021] All rights reserved.

Manuscript submitted July 8, 2003; revised manuscript received August 25, 2003 Available electronically January 9, 2004.

Considerable efforts have been devoted to the synthesis, understanding physicochemical properties, and exploiting conjugated organic polymers in various applications.<sup>1-4</sup> Numerous studies on the growth of various conducting polymers such as polyaniline, polypyrrole, polythiophene, and polyfluorenes (PFIs) have been reported for a better understanding of the roles played by various experimental parameters for their growth.<sup>5-20</sup> Increasing interest in the electrosynthesis of nanoscale/tubular materials, have added new dimensions to the field of electrochemical synthesis of conducting polymers.<sup>21,22</sup> Studies on the polymer growth mechanism, kinetics of the polymerization reaction rate, and associated quantitative characteristics of polymerization of polyaniline, poly(3-methylthiophene), and polypyrrole have also been conducted using cyclic voltammetric, electrochemical quartz crystal microbalance (EQCM), and spectroelectrochemical techniques.<sup>23-27</sup>

PFIs are an important class of electroactive and photoactive materials known to emit photons spanning the entire visible range with high efficiencies and low operating voltages and also exhibit unusual properties such as thermochromism.<sup>2,3</sup> Fluorene is a biphenyl derivative, in which the ortho carbon atoms of the two benzene rings are bridged by a methylene group. A few different PFIs, as well as fluorene-based copolymers and homopolymers, have been synthesized chemically and electrochemically from fluorene and its 9- or 9,9-derivatives and studied for their physicochemical properties in last two decades.<sup>28-43</sup> Attractive features of 9,9-disubstituted PFIs are that they can exist in three redox states, p-doped, neutral, and n-doped. PFIs, in general, have been subjected to a variety of applications such as electrochromic materials, in batteries, cation complexing materials, organic light emitting diodes, and also as electrode surface modifiers.<sup>2,3,30-32,44</sup>

Conducting polymers are prepared by chemical or electrochemical oxidation of monomeric compounds.<sup>1,6,18</sup> Electrochemical methods of preparation include potentiostatic, potentiodynamic, and galvanostatic experiments.<sup>1,18</sup> The potentiodynamic method is reported to produce films with superior adhesion, smoothness, and optical properties.<sup>45-47</sup> PFI films obtained by constant potential electrolysis were brittle and hydrogen rich with electrical conductivity of  $10^{-4}$  S/cm. Rault-Berthelot *et al.* have also reported anodic polymerization and spectroelectrochemical studies on PFI in

$\text{CH}_3\text{CN}$ .<sup>29-31</sup> Two charged species, cation radicals and dications, are produced during anodic polymerization. The mode of polymerization concerns C-C linkage formation through aromatic carbon atoms and does not involve the  $>\text{CH}_2$  group because fluorene with methyl and dimethyl substituents on the methylene group led to identical polymers.

We report here results of our systematic studies of the effects of solvents, polymer growth kinetics, and growth efficiencies employing cyclic voltammetry, electrochemical quartz crystal microbalance (EQCM), and spectroelectrochemical techniques under potentiodynamic conditions to gain a better understanding of the parameters determining the quality of the polymer film.

### Experimental

Fluorene, tetrabutylammonium tetrafluoroborate (both Aldrich, 99%),  $\text{CH}_2\text{Cl}_2$ , and  $\text{CH}_3\text{CN}$  (both Fluka, anhydrous grade) were used as received. A platinum disk (diam. 1 mm), a silver wire in  $\text{AgNO}_3$  (0.10 M  $\text{AgNO}_3$  in  $\text{CH}_3\text{CN}$ ), and a platinum strip were used as working, reference, and counter electrodes, respectively. A three-compartment electrochemical cell, in which the counter and working electrode compartments were separated by a glass frit, was employed. The working electrode was polished with 1.0, 0.3, and 0.05  $\mu\text{m}$  alumina slurry (Fisher), washed with deionized water and acetone, and dried prior to each experiment. Fresh monomer and supporting electrolyte solutions were prepared prior to each experiment. Oxygen was removed by purging the solution with high purity argon gas prior to the experiments, and the argon atmosphere was maintained over the solution during the course of the experiments.

The EQCM measurements were carried out using a Seiko EG&G model 917 quartz crystal analyzer (QCA) along with an EG&G model 273 potentiostat/galvanostat. An AT-cut, 9 MHz platinum-plated quartz crystal (Seiko EG&G model QA-A9M-Au, 0.20  $\text{cm}^2$ ) was used as a resonator and an electrode. The platinum-coated quartz crystal working electrode was mounted on a model QA-CL3 electrode holder. The QCA, the potentiostat/galvanostat, and the computer were connected through a GPIB interface card, which was controlled by EG&G 270/250 electrochemistry software. The sensitivity of the quartz crystal electrode was calibrated by potentiostatic deposition of silver from a silver nitrate solution. *In situ* ultraviolet-visible (UV-vis) spectra were taken with an Oriel InstaSpec IV spectrometer with a charge-coupled device (CCD) array detector, which was configured in a near normal incidence reflectance mode using a bifurcated quartz optical fiber.<sup>48,49</sup> The wavelength of the spectrophotograph was calibrated using a small mercury lamp.

\* Electrochemical Society Active Member.

<sup>a</sup> Present address: BARC, Fuel Chemistry Division, Mumbai 400 085, India.

<sup>z</sup> E-mail: smpark@postech.edu

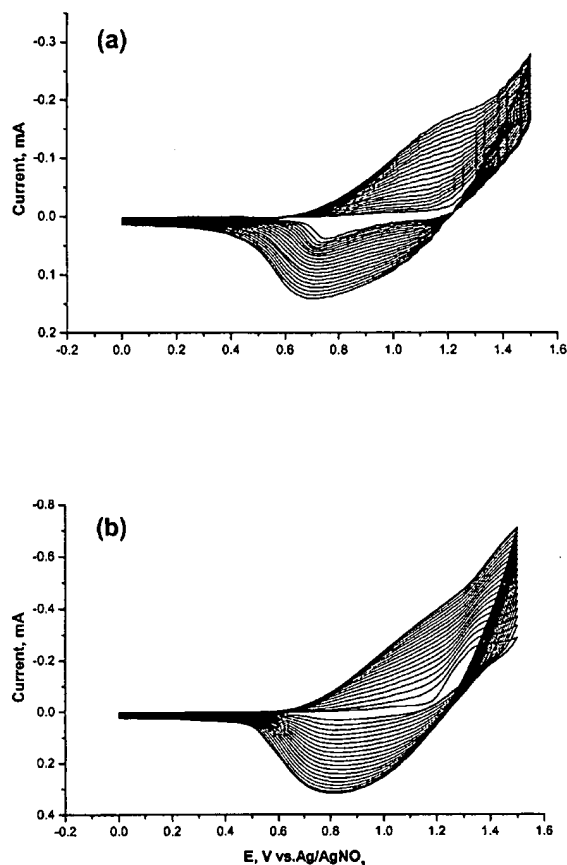


Figure 1. A series of cyclic voltammograms recorded from a solution containing 0.010 M fluorene and 0.20 M TBA- $\text{BF}_4$  solution at a scan rate of 100 mV/s in (a)  $\text{CH}_2\text{Cl}_2$  and (b)  $\text{CH}_3\text{CN}$ .

### Results and Discussion

**Polyfluorene growth in  $\text{CH}_2\text{Cl}_2$  and  $\text{CH}_3\text{CN}$ : Potentiodynamic studies.**—Figure 1 shows a series of 20 cyclic voltammograms (CVs) recorded during PF1 growth in  $\text{CH}_2\text{Cl}_2$  and  $\text{CH}_3\text{CN}$ . Noticeable features observed from the CV studies were: the onset potentials are observed at  $\sim 1.2$  V for monomer oxidation in the first forward scan in both solvents but relatively higher oxidation currents were observed in  $\text{CH}_3\text{CN}$  than in  $\text{CH}_2\text{Cl}_2$ . The CVs recorded in both solvents indicate that  $\text{CH}_2\text{Cl}_2$  was more resistive than  $\text{CH}_3\text{CN}$  and, thus, required larger overpotentials for oxidation of both the monomer and the polymer. The general characteristics of the electrochemical polymerization of fluorene and the potentials observed here for oxidation of the monomer are in good agreement with those reported previously.<sup>28-30</sup>

**Kinetic studies.**—Studies on the polymerization kinetics were carried out in  $\text{CH}_2\text{Cl}_2$  and  $\text{CH}_3\text{CN}$  to understand effects of various experimental parameters on the growth of PF1, and the results are shown in Fig. 2. There, cathodic charges accumulated ( $Q$ ) due to reduction of the polymer film during the reverse scan were taken as a measure of polymer growth on the electrode surface.<sup>14,23</sup> The  $Q$  values were determined by integrating the cathodic current in each cyclic voltammogram and have been plotted as a function of the potential cycle number (CN) at different fluorene concentrations for both the solvents. As can be seen,  $Q$  increased with the increase of the CN as well as with the increase of the monomer concentration in

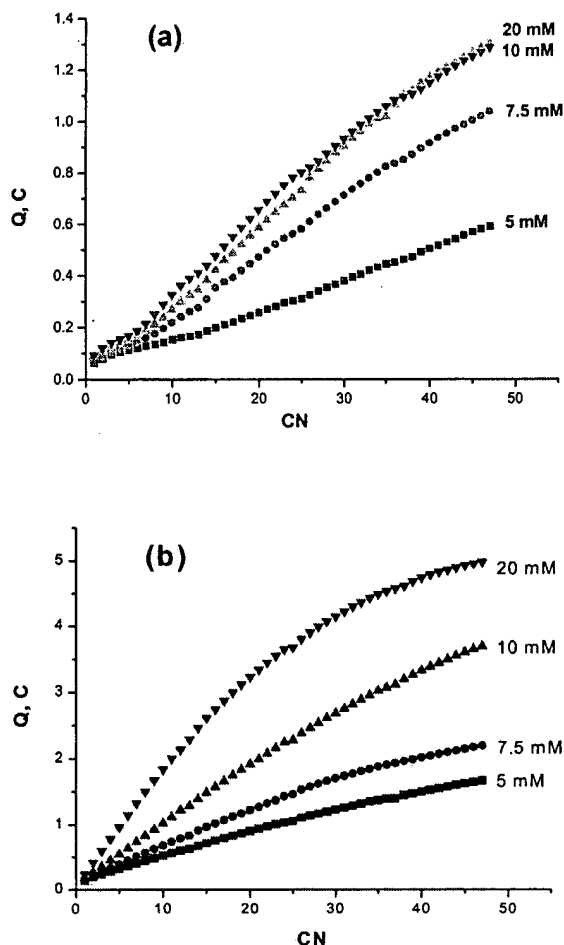


Figure 2. The cathodic charge ( $Q$ ) plotted as a function of the cycle number (CN) in: (a)  $\text{CH}_2\text{Cl}_2$ , (b)  $\text{CH}_3\text{CN}$ . The data were taken from 48 consecutive cyclic voltammograms at different monomer concentrations under otherwise identical conditions as those used for Fig. 1. The monomer concentrations are marked on the figure.

both the solvents, indicating that the polymer film was growing. The growth rate with respect to the scan number, *i.e.*,  $dQ/d(\text{CN})$ , is plotted in Fig. 3. These plots (Fig. 3a) indicate that the growth rates decreased as the number of potential scans increased in  $\text{CH}_3\text{CN}$ . The decrease was more pronounced at higher monomer concentrations, suggesting that the polymer film got increasingly less conductive as the film became thicker. This behavior should result from the increase in the electrical resistance and the resistance to mass transport through the film as the film became thicker.

Note that the growth pattern in  $\text{CH}_2\text{Cl}_2$  is totally different from that in  $\text{CH}_3\text{CN}$ . First, the growth rates are much smaller in  $\text{CH}_2\text{Cl}_2$  than in  $\text{CH}_3\text{CN}$ , ranging anywhere between about 1/6 to 1/3 of those in  $\text{CH}_3\text{CN}$  depending on the monomer concentrations and the potential cycle numbers. Second, the rates fluctuate more or less periodically in both  $\text{CH}_2\text{Cl}_2$  and  $\text{CH}_3\text{CN}$  as the number of potential cycles increases, although the fluctuation is more severe in  $\text{CH}_2\text{Cl}_2$ . Dichloromethane is a nonpolar solvent compared to  $\text{CH}_3\text{CN}$  and, thus, would dissolve the oligomers better than  $\text{CH}_3\text{CN}$ , resulting in smaller rates of film growth particularly in earlier stages. This would result in an accumulation of a smaller amount of oligomers on the surface, but the smaller amounts of oligomers deposited on the surface appear to passivate the electrode as well, due to their poor

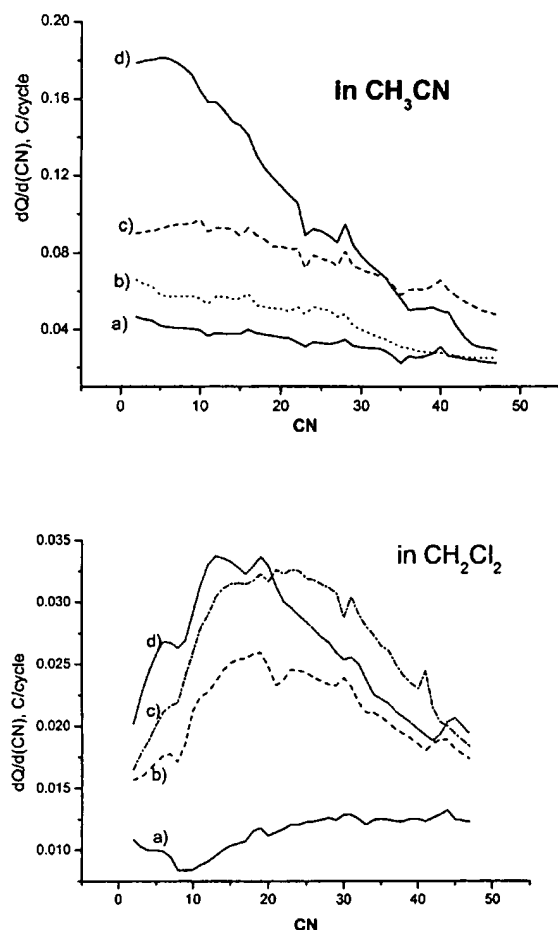


Figure 3. The  $dQ/d(CN)$  plotted as a function of cycle number (CN) in  $CH_3CN$  (above) and  $CH_2Cl_2$  (below) at a fluorene concentration of: (a) 0.005 M, (b) 0.0075 M, (c) 0.01 and (d) 0.02 M. Data were taken from Fig. 2.

electrical conductivity and the bulky counter anions (see the EQCM results below). When an electrode is covered with organic salts having bulky anions, the electrode would be passivated. In later stages, however, the passivation would become less severe as the oligomers would have grown to more conductive polymers on the electrode surface unless the film thickness is excessively large such as the case in which the monomer concentration is 20 mM. Thus, as the polymer chain grows, the film becomes more conductive, and the growth rate increases significantly until about the 20th cycle, when it starts to decrease again (Fig. 3b). At this point, both the electrical resistance through the film and the resistance to mass transport becomes a major obstacle to fast growth. This explains at least qualitatively the shape of growth rates shown in Fig. 3.

Unfortunately, we could not extract the other kinetic information such as reaction orders from the data shown in Fig. 2 and 3 in the same way as has been done on the other polymerization reactions.<sup>14,23,25</sup> However, we concluded from the observations that the polymerization reaction was more effective in a polar solvent such as  $CH_3CN$ . While the films grown in  $CH_3CN$  showed somewhat increased film resistance due to the increases in film thickness in later stages of the polymer growth, the films grown in  $CH_2Cl_2$  passivated the surface effectively due perhaps to smaller chain lengths, rendering the film less conductive.

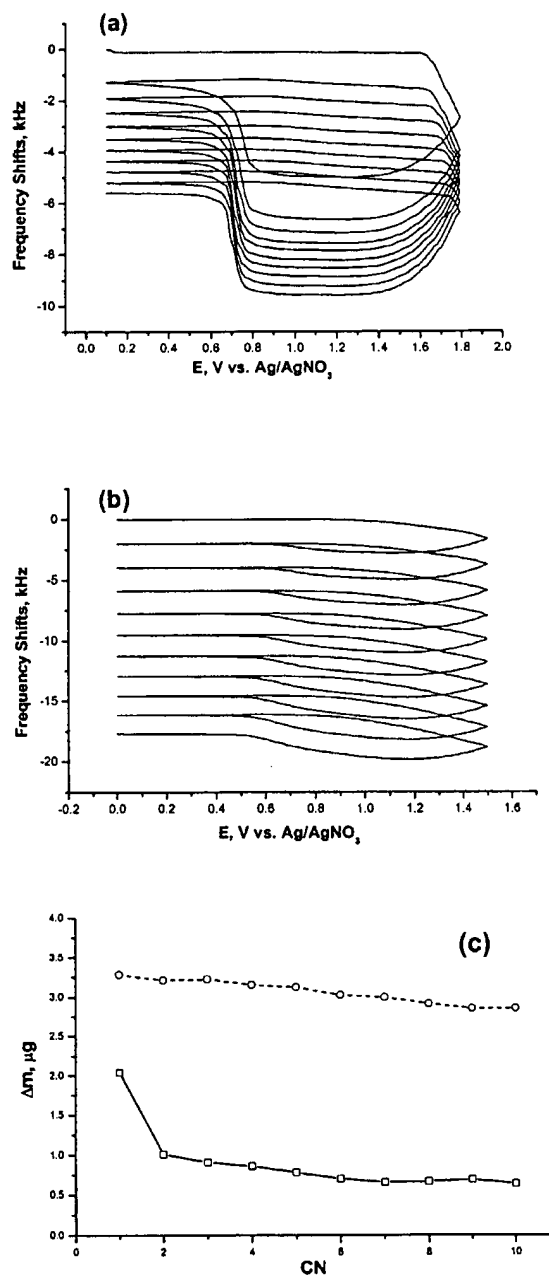


Figure 4. Frequency shifts recorded during PFI growth in a 0.010 M fluorene + 0.20 M TBA-BF<sub>4</sub> solution in (a)  $CH_2Cl_2$  and (b)  $CH_3CN$ , and (c) The amount of PFI ( $\Delta m$ ) deposited on the electrode as a function of cycle number (CN) in (□)  $CH_2Cl_2$  and (○)  $CH_3CN$ . The potential was cycled at a scan rate of 100 mV/s in the 0.1–1.8 V range in  $CH_2Cl_2$  but 0.0–1.5 V in  $CH_3CN$ .

**EQCM studies.**—Figure 4 shows typical results obtained from EQCM experiments during potentiodynamic scanning in (a)  $CH_2Cl_2$  and (b)  $CH_3CN$ , and (c) the summary of the results in both solvents. The same trends as those observed during the growth experiments are observed here in that (i) the amounts of the polymer deposited in  $CH_3CN$  are about 3–4 times of those in  $CH_2Cl_2$  (Fig. 4c) and (ii) the

Table 1. Net charges utilized, corresponding changes in frequency, amounts of PF1 deposited, and the apparent number of electrons transferred for each fluorene monomer unit deposited during potentiodynamic growth of PF1, under the experimental conditions shown in Fig. 4.

CN	Dichloromethane				Acetonitrile			
	$Q_{\text{net}}$ ( $\mu\text{C}$ )	$\Delta(\Delta F)$ (Hz)	$\Delta m$ ( $\mu\text{g}$ )	$n_{\text{app}}$	$Q_{\text{net}}$ ( $\mu\text{C}$ )	$\Delta(\Delta F)$ (Hz)	$\Delta m$ ( $\mu\text{g}$ )	$n_{\text{app}}$
1	1882	1278	2.04	1.6	3314	2052	3.28	1.7
2	1952	634	1.01	3.3	3142	2008	3.21	1.7
3	1966	566	0.91	3.7	3160	2010	3.22	1.7
4	1981	536	0.86	4.0	3105	1970	3.15	1.7
5	1982	490	0.78	4.4	3093	1950	3.12	1.7
6	1985	438	0.70	4.9	3080	1890	3.02	1.8
7	1984	410	0.66	5.2	3070	1870	2.99	1.8
8	1985	420	0.67	5.1	3058	1820	2.91	1.8
9	1981	430	0.69	5.0	3054	1780	2.85	1.8
10	1982	400	0.64	5.3	3043	1780	2.85	1.8

rate of accumulation decreased in  $\text{CH}_2\text{Cl}_2$  as the cycle number increased, although the rate of increase in charge increased for the first 10 cycles (Fig. 3c in  $\text{CH}_2\text{Cl}_2$ ). This indicates that the current efficiency decreased drastically as the number of potential cycles increased. This is also shown in  $n_{\text{app}}$  listed in Table 1; more on this is discussed below. Similar observations have been reported on electrochemical synthesis of polyaniline.<sup>50</sup>

We also note that the amount of the deposit left on the surface upon returning the potential back to 0.10 V was only 25% of the initially deposited total weight deposited in  $\text{CH}_2\text{Cl}_2$ , while it was about 85% in  $\text{CH}_3\text{CN}$ . This trend continued until the tenth potential cycle as can be seen from Fig. 4a and b. This is explained by the fact that the polymerization reaction was much more effective, resulting in the more conductive polymer formation in  $\text{CH}_3\text{CN}$  than in  $\text{CH}_2\text{Cl}_2$  as noted earlier during the discussion of the results obtained from the kinetic experiments. The large weight loss in  $\text{CH}_2\text{Cl}_2$  must have been due to the effective dissolution of a large amount of neutral oligomers produced upon returning to 0.10 V, which had large ion pairs incorporated into their oxidized states (see below). The effective dissolution of the deposit would result from smaller chain lengths of the oligomers. That these oligomers had smaller chain lengths is shown by the poor conductivity of the films as was shown during the polymer growth and also by the shorter wavelengths at which they absorb (see below).

The large weight losses of about 75% upon returning the potential to 0.10 V are attributed to the ejection of the incorporated ion pair as large as  $(\text{TBA})_4(\text{BF}_4)_5^-$ , rather than bare  $\text{BF}_4^-$ , into the oxidized oligomers, which are reduced to the neutral species during the cathodic scan. Assuming that the doping level of this polymer is such that a positive charge is shared by three monomer units in the oxidized polymer or oligomers, an ejection of the counter ion pair,  $(\text{TBA})_4(\text{BF}_4)_5^-$ , from the doped oligomer or polymer, *i.e.*,  $(\text{Fl})_3^+ - (\text{TBA})_4(\text{BF}_4)_5^-$ , would account for a 25% retention of the neutral polymer or 75% of weight loss if only the ejection of the counter anion leads to the weight loss upon reduction of the oxidized polymer or oligomer.

Approximately 2-5 monomer molecules are known to share a positive charge when conducting polymers are doped, although the doping level depends on the type of polymer, the film thickness, and other parameters.<sup>51</sup> This would happen because the charge-to-weight ratio of the oxidized oligomers must be small in  $\text{CH}_2\text{Cl}_2$  due to its low dielectric constant ( $\epsilon = 9.08$ ) in comparison to that of  $\text{CH}_3\text{CN}$  ( $\epsilon = 37.5$ ). Ions are more stable when they form large ion pairs in associative, low dielectric media such as  $\text{CH}_2\text{Cl}_2$ .

In  $\text{CH}_3\text{CN}$ , however, the primary oxidation product of the monomer (radical cation) undergoes rapid polymerization as is evidenced by the results obtained from polymer growth, EQCM, and spectroelectrochemical experiments (see below). The weight loss of about 15% upon reversing the potential to 0.0 V during the cathodic scan

corresponds to a loss of an anion for every three fluorene monomer units and this is consistent with the approximate doping level of typical conducting polymers, *i.e.*,  $(\text{Fl})_3^+ - \text{BF}_4^-$ . Thus, our EQCM results allow us to estimate not only the doping level of the polymer but also the average size of counter ion pairs.

Figure 5 shows the  $-d\Delta F/dt$  curves for the first EQCM profile (Fig. 4a and b) along with CVs obtained concurrently with the EQCM data in the two solvents. The  $d\Delta F/dt$  curves should have an identical shape with the corresponding CVs if the precipitation results directly from the primary product of the electrochemical process with all the charges consumed for its deposition. It can be seen

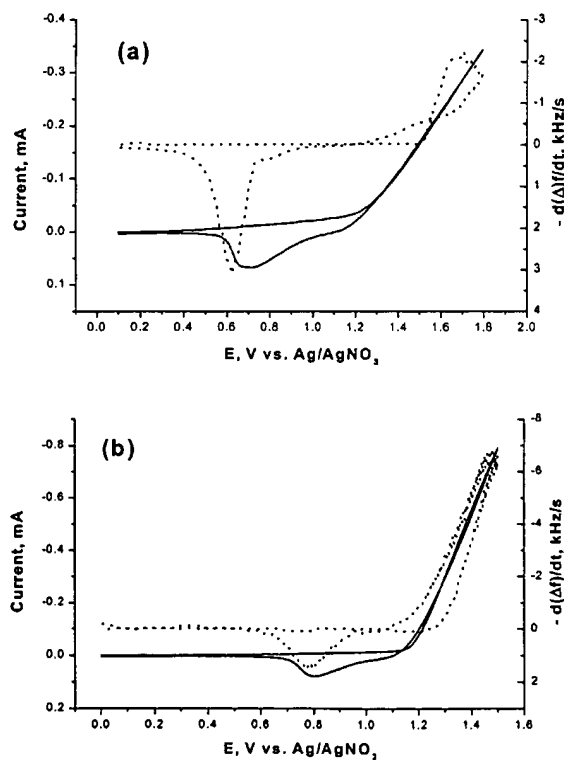


Figure 5. The  $-d(\Delta f)/dt$  plots obtained from the  $\Delta f$  vs.  $E$  plots shown in Fig. 4a and b for the first potential cycle in (a)  $\text{CH}_2\text{Cl}_2$  and (b)  $\text{CH}_3\text{CN}$ . Dotted lines display  $-d(\Delta f)/dt$  curves while the solid lines show CVs recorded during the first cycle.

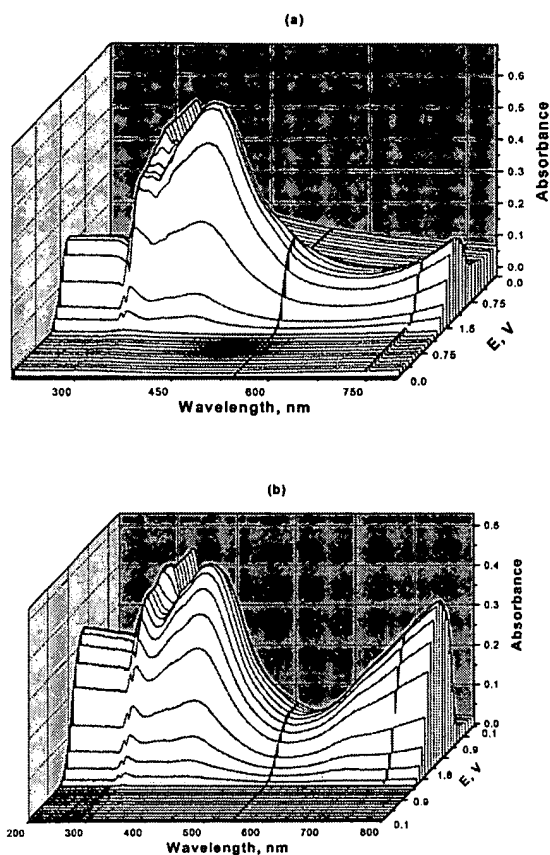


Figure 6. *In situ* UV-vis absorption spectra recorded during PFI growth at a platinum electrode between (a) 0.0 and 1.5 V in  $\text{CH}_3\text{CN}$ , and (b) 0.10 and 1.8 V in  $\text{CH}_2\text{Cl}_2$ . The potential sweep rate was 100 mV/s.

from the figure that the maximum deposition rate of the film was about 2.2 kHz/s in  $\text{CH}_2\text{Cl}_2$  while it was about 6.5 kHz/s in  $\text{CH}_3\text{CN}$  and the ratio of the deposition rates in the two solvents was about the same as was observed during the growth rate experiments. The delays observed between the onset potentials for the current increase and the frequency decrease indicate that the deposit resulted from the following chemical reactions of the primary electrochemical product, *i.e.*, radical cations. These delays were about 300 and 100 mV, respectively, in  $\text{CH}_2\text{Cl}_2$  and  $\text{CH}_3\text{CN}$ . This is because: (i) the film prepared in  $\text{CH}_2\text{Cl}_2$  was more resistive than that in  $\text{CH}_3\text{CN}$ , (ii) the  $\text{CH}_2\text{Cl}_2$  solution was a more associative solvent than  $\text{CH}_3\text{CN}$ , and (iii) the electrochemical reaction was more reversible in  $\text{CH}_3\text{CN}$  than in  $\text{CH}_2\text{Cl}_2$ .

Quantitative results obtained from CV-EQCM experiments on polymer growth in the two solvents are listed in Table I. Here net charges,  $Q_{\text{net}}$ , were obtained from the differences in charge after a potential cycle is completed. Using  $Q_{\text{net}}$  and the amount of the PFI films calculated using the Sauerbrey equation,<sup>52</sup> the number of electrons transferred per monomer ( $n_{\text{app}}$  values), which is the number of electrons required to deposit a mole of fluorene monomer unit, was evaluated for each CN in both solvents. The  $n_{\text{app}}$  values range between 1.7 and 1.8 in  $\text{CH}_3\text{CN}$ , while they are in the range of 1.6 and 5.3 in  $\text{CH}_2\text{Cl}_2$ . This indicates that the coulombic efficiency of the oxidative polymerization is about 100% in A CN assuming a stoichiometry

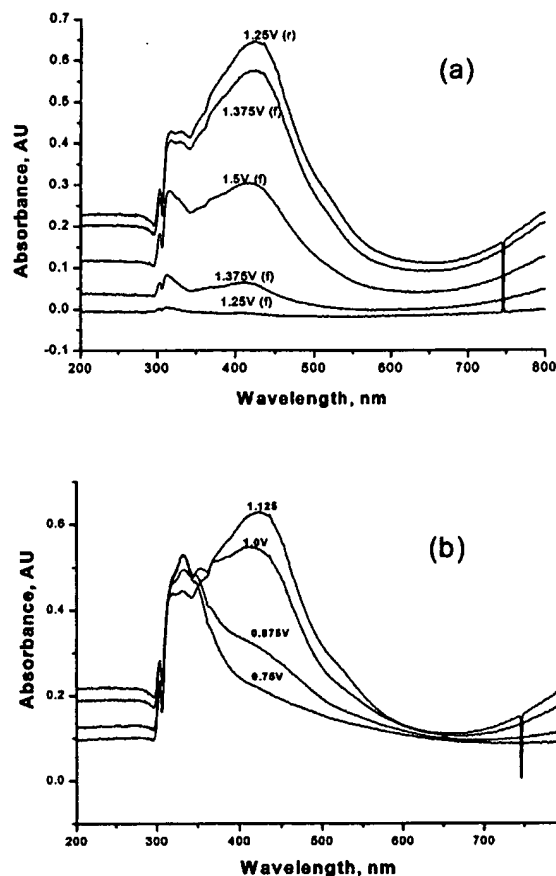
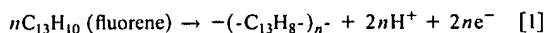


Figure 7. A few absorption spectra depicting PFI growth during the forward (a) and reverse (b) scans of the first CV sweep at various anodic potentials in  $\text{CH}_3\text{CN}$ . The spectra have been taken from Fig. 6a. The forward (f) and reverse (r) scan directions are indicated in parentheses in a.

while it is anywhere between 37% and 100% in  $\text{CH}_2\text{Cl}_2$  depending on the number of potential cycles. The reason why the  $n_{\text{app}}$  values are smaller than 2.0 is probably because the counter anions are not completely ejected from the film after the potential returns to the initial value. Waltman *et al.*<sup>31</sup> have reported an “*n*” value of 2.5 for PFI growth in  $\text{CH}_3\text{CN}$ , under potentiostatic conditions. The rapid drop in coulombic efficiencies in  $\text{CH}_2\text{Cl}_2$  should be due to the poor film conductivity as already pointed out.

**Spectroelectrochemical studies.**—Figure 6 shows a series of UV-vis spectra recorded during the growth of PFI in  $\text{CH}_2\text{Cl}_2$  and  $\text{CH}_3\text{CN}$ , respectively, under the experimental conditions shown in Fig. 4. Each absorption spectrum was recorded in a 25 mV potential interval. The reflectance spectrum recorded at 0.0 V was used as a reference for calculation of absorbance and, thus, the absorbance signals displayed in the absorption spectra were the difference spectra arising from the electrolysis of monomers during the potential scan.

It is seen from Fig. 6 that no absorption bands are observed in  $\text{CH}_3\text{CN}$  until the potential reaches  $\sim 1.25$  V, where oxidation of fluorene monomers commences. Afterward three bands, namely at about 314 nm, 410 nm, and a wavelength longer than 800 nm, are seen to grow. Fluorene absorbs at about 260 nm in  $\text{CH}_3\text{CN}$  and the absorption band at 314 nm observed here is closer to the one reported for PFI (325 nm).<sup>31</sup> We assigned the 314 nm band to rela-

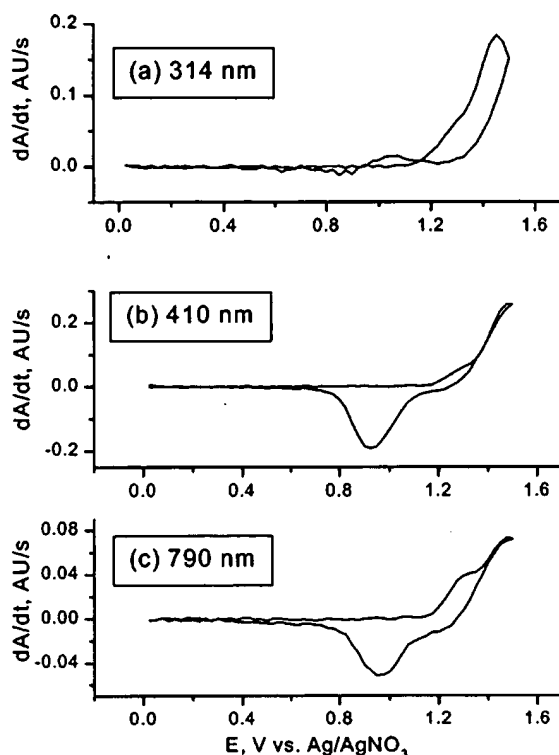


Figure 8. DCVA curves for the data shown in Fig. 6a for PFI growth in  $\text{CH}_3\text{CN}$  at (a) 314 nm, (b) 410 nm, and (c) 790 nm.

tively shorter chain polymers generated during an early stage of polymerization.<sup>31</sup> Initially this peak grew appreciably during the forward scan and shifted to longer wavelengths as the potential got more anodic, which is an indication of polymer growth as the potential got more anodic. At the same time, the 410 nm band grew at a relatively faster rate from 1.38 V in the forward scan back to 1.25 V in the reverse scan and showed a sharp decrease in intensity at potentials more cathodic than 1.13 V (Fig. 7). This suggests that the species absorbing at 410 nm were the first oxidized species of the polymer. Note in Fig. 7b that while the intensity of the 410 nm band appreciably decreased from 1.13 V in reverse scan, the intensity of the 314 nm band showed an increase at its expense and an isosbestic point was observed at about 350 nm (Fig. 7b), albeit not very clearly. This indicates that the species absorbing at 314 nm are generated at the cost of that absorbing at 410 nm during the reversal scan. This points to the fact that the species absorbing at 314 and 410 nm were a redox pair with electrons exchanged between the two species. We thus assigned the 410 nm band to radical cations of long chain oligomers or short chain polymers. It can also be noted that the intensity of the longer wavelength band increased appreciably in the subsequent CV scans as compared to that of first (not shown). We assigned the longer wavelength band to the dication radical or bipolaron. Finally, we notice that the 314 and 410 nm bands were red shifted to about 334 and 427 nm by the time the reversal potential scan is completed. All the absorption bands underwent red shifts in successive scans suggesting that the polymer grew continuously, although the shifts converge to certain values.

Similar behaviors were observed during the PFI growth in  $\text{CH}_2\text{Cl}_2$  as can be seen in Fig. 6b except that the corresponding bands are observed at shorter wavelengths than those in  $\text{CH}_3\text{CN}$ , i.e., 306 nm, 392 nm, and the longer wavelength band. This suggests that the conjugation length of the oligomers generated during the

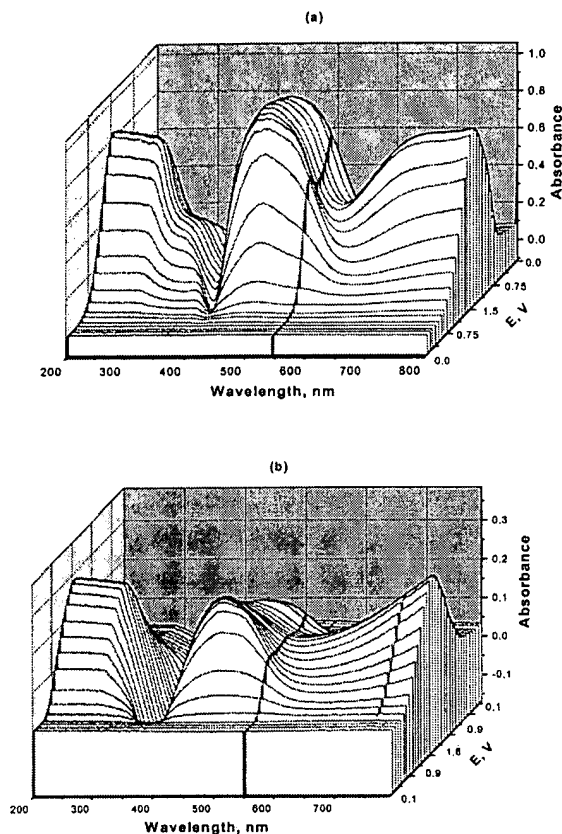


Figure 9. *In situ* UV-vis absorption spectra recorded from PFI films during the potential scan at a scan rate of 100 mV/s without monomers in (a)  $\text{CH}_3\text{CN}$  from 0.0 to 1.5 V and back to 0.0 V and (b)  $\text{CH}_2\text{Cl}_2$  from 0.1 to 1.8 V and back to 0.1 V.

early period of polymerization was significantly smaller in  $\text{CH}_2\text{Cl}_2$  as compared to those in  $\text{CH}_3\text{CN}$ .

Because the spectra shown in Fig. 6 are highly crowded and, thus, it is difficult to see how each band behaved during the potential sweep, we have plotted the rates of increase/decrease in absorbance ( $dA/dt$ ) at given wavelengths as a function of the potential, which is termed derivative cyclic voltabsorptometry (DCVA).<sup>14,26,49</sup> The DCVA signals obtained at 314, 410, and 790 nm from the data shown in Fig. 6a are displayed in Fig. 8. The DCVA curve obtained at 314 nm (Fig. 8a) shows that the species absorbing at that wavelength was produced in a large quantity as soon as fluorene oxidation commenced, and its maximum rate of generation was observed at  $\sim 1.45$  V but then decreased beyond this potential. That species is a nonreducible compound within the potential sweep limit used in this experiment.

The DCVA curve at 410 nm (Fig. 8b) shows that the species absorbing at that wavelength was produced in large quantities at around 1.48 V, and then its rate also decreased rapidly and became negative below 1.2 V upon reversing the scan. The negative signal resulted from the reduction of the radical cations of oligomers. The DCVA curve for the species absorbing at 790 nm (Fig. 8c) behaved in a similar way but appeared to be generated at the expense of the 410 nm band above about 1.25 V. We thus assign this band to the bipolaron of the oligomers. The DCVA curves for the corresponding bands recorded in  $\text{CH}_2\text{Cl}_2$  (not shown) behaved similarly.

Figure 9 shows a series of absorption spectra recorded for the PFI film deposited on the Pt electrode in monomer-free  $\text{CH}_3\text{CN}$  (a)

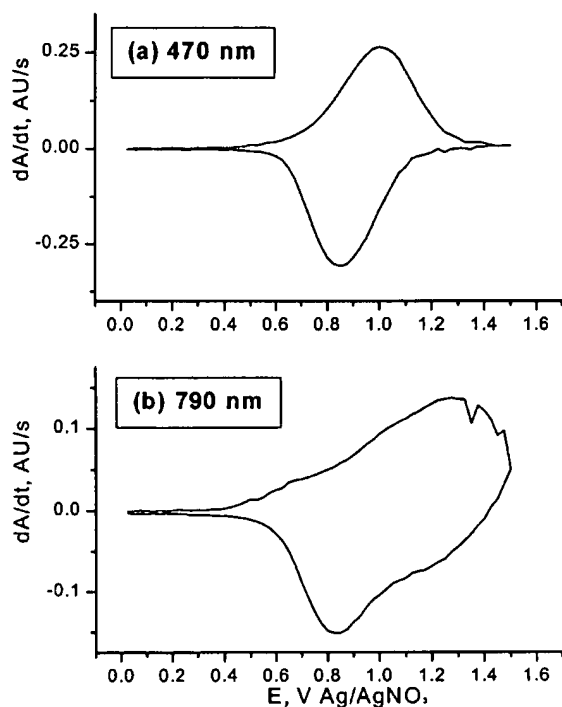


Figure 10. DCVA curves obtained for the data shown in Fig. 9a at 470 and 790 nm.

and  $\text{CH}_2\text{Cl}_2$  (b) electrolyte solutions. In efforts to see the spectral changes more clearly, we again show the DCVA curves for the bands corresponding to polarons and bipolarons at 470 and 790 nm in both  $\text{CH}_3\text{CN}$  (Fig. 10) and  $\text{CH}_2\text{Cl}_2$  (not shown) solutions, respectively. It is seen from Fig. 10 that the bipolaron began to be generated at the same time or potential when the polaron is being generated. This is due to the disproportionation reaction



The DCVA at 470 nm shown in Fig. 10a indicates that the neutral PFI underwent a reversible electron transfer reaction to produce a polaronic species with its anodic and cathodic peak potentials of  $\sim 0.97$  and  $\sim 0.86$  V, respectively. However, the DCVA curve recorded at 790 nm behaved differently, in that it was generated as soon as the polaron was being generated with its anodic peak potential ( $E_p = \sim 1.25$  V) well beyond the peak potential for the generation of the polaronic species ( $E_p = \sim 0.97$  V). This suggests that the bipolaron was generated slowly not only as a result of the disproportionation reaction as shown above but also via direct oxidation of polarons at a slightly higher potential. Similar behaviors were observed for the PFI film prepared in dichloromethane except that the first reaction was not as reversible as that for the film prepared in  $\text{CH}_3\text{CN}$ .

Finally, it should be pointed out from Fig. 9 that the bipolaron transition starting above 700 nm was quite strong in PFI films prepared in  $\text{CH}_3\text{CN}$  compared to those in  $\text{CH}_2\text{Cl}_2$ , indicating that the conductivity of the doped polymer would also be significantly higher in  $\text{CH}_3\text{CN}$ . This should also be due to the longer chain lengths of the film prepared in  $\text{CH}_3\text{CN}$ .

**Morphology of PFI films.**—Figure 11 shows scanning electron microscopy images of PFI films prepared at QCA electrodes in  $\text{CH}_3\text{CN}$  (a and b) and in  $\text{CH}_2\text{Cl}_2$  (c). It is seen that the PFI film grew uniformly covering the whole electrode surface with small polymer

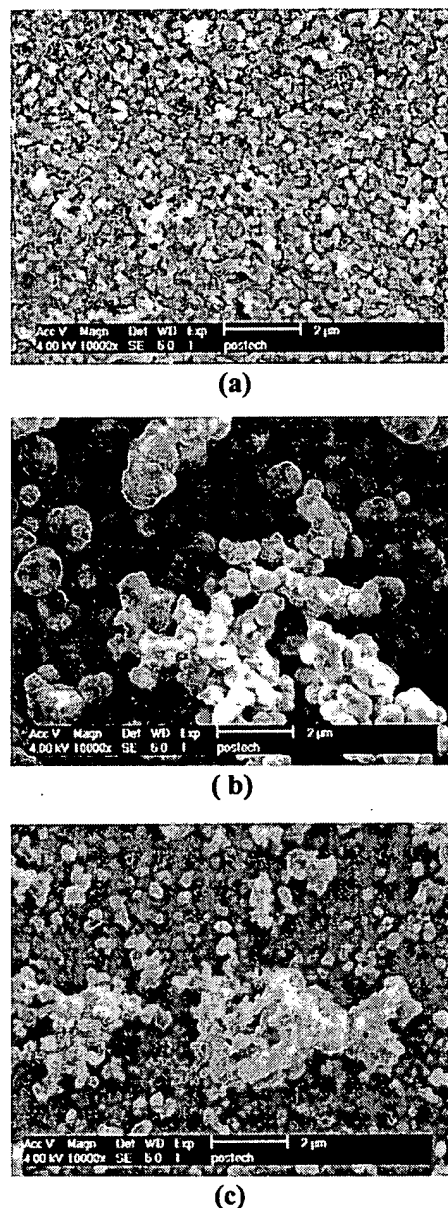


Figure 11. SEM images obtained from PFI films grown potentiodynamically (a) after 5 CV scans in  $\text{CH}_3\text{CN}$ , (b) 15 CV scans in  $\text{CH}_3\text{CN}$ , and (c) 15 CV scans in  $\text{CH}_2\text{Cl}_2$ .

grains of about 50–150 nm from the beginning (Fig. 11a) but they later grew to larger lumps as large as about 600–700 nm at certain locations (Fig. 11b). In  $\text{CH}_2\text{Cl}_2$ , however, PFI growth was not as uniform and slow even after the 15th CV scan. Perhaps the surface where the polymer grains were not found might have been passivated due to the deposition of small oligomers during the early phase of the polymerization reaction. Those areas not only hindered further growth of the polymer but also rendered the spots less conductive.

### Conclusion

Our results show clearly the role of solvents in electrochemical polymerization of nonpolar compounds such as fluorene. The poly-



merization reaction was much more efficient in a polar solvent such as  $\text{CH}_3\text{CN}$  thanks to their high solvent conductivity, strong dissociative properties, and stabilization of doped polymers in comparison to that in  $\text{CH}_2\text{Cl}_2$ . From the EQCM measurements, we demonstrated that the counteranions must be in the form of ion pairs such as  $(\text{TBA})_4(\text{BF}_4)_3^-$  rather than bare anions,  $\text{BF}_4^-$ . To our knowledge this is the first description of the heavily associated ion pairs, which should allow many anomalous observations reported hitherto in the literature to be interpreted correctly.<sup>30</sup> This also explains why the nonpolar polymers such as PPP do not grow efficiently in nonpolar solvents even though those solvents must be used to increase the solubility of such monomers. The EQCM measurements were also shown to allow the doping levels to be estimated in our study and the weight loss estimated fits in our postulate rather nicely. The insights gained in our study regarding the parameters for preparing conducting polymers would provide guidelines for choosing optimum conditions, under which better conducting polymers are obtained.

### Acknowledgments

The visiting scholarship was provided to H.S.S. by the BK-21 program of the Ministry of Education of Korea and the research was supported by the Korea Science and Engineering Foundation through the Center for Integrated Molecular Systems of POSTECH. Thanks are also due to Dr. V. Venugopal, Head, FCD, Shri D.S.C. Purushotham and Shri H. S. Kamath, former and present Director, NFG, BARC, India, for their encouragement and keen interest in this work. H.S.S. is indebted to Dr. S. K. Aggarwal, Head MS Section, FCD, BARC for his innovative advice to work in the area of conductive polymers and constant support during the course of this work.

Pohang University of Science and Technology assisted in meeting the publication costs of this article.

### References

1. S.-M. Park, in *Handbook of Organic Conductive Molecules and Polymers*, Vol. 3, H. S. Nalwa, Editor, John Wiley & Sons, Chichester, England (1997).
2. J. Rault-Berthelot, *Recent Res. Devel. Macromol. Res.*, **3**, 425 (1998).
3. M. Leclerc, *J. Polym. Sci., Part A: Polym. Chem.*, **39**, 2867 (2001).
4. H. Shirakawa, A. G. MacDiarmid, and A. J. Heeger, *Chem. Commun. (Cambridge)*, **2003**, 1.
5. D. Orata and D. A. Buttry, *J. Am. Chem. Soc.*, **109**, 3574 (1987).
6. C. R. Martin, *Acc. Chem. Res.*, **28**, 61 (1995).
7. B. Nossakh, Z. K. Machnik, and F. Tedjar, *J. Electroanal. Chem. Interfacial Electrochem.*, **269**, 263 (1990).
8. H. Yang, D. O. Wipf, and A. J. Bard, *J. Electroanal. Chem.*, **331**, 913 (1992).
9. L. Duic, Z. Mandic, and S. Kovac, *Electrochim. Acta*, **40**, 1681 (1995).
10. T. Osaka, T. Nakajima, K. Shiota, and T. Momma, *J. Electrochem. Soc.*, **138**, 2853 (1991).
11. R. V. Parthasarathy and C. R. Martin, *Chem. Mater.*, **6**, 1627 (1994).
12. N. Kuramoto, J. C. Michaelson, A. J. McEvoy, and M. Gratzel, *J. Chem. Soc., Chem. Commun.*, **1990**, 1478.
13. S. K. Dhawan and D. C. Trivedi, *J. Appl. Electrochem.*, **22**, 563 (1992).
14. S. N. Hoier and S.-M. Park, *J. Electrochem. Soc.*, **140**, 2454 (1993).
15. S. Prumeanu, E. Csahok, V. Kertesz, and G. Inzelt, *Electrochim. Acta*, **43**, 2305 (1998).
16. S. Ramirez and A. R. Hilman, *J. Electrochem. Soc.*, **145**, 2640 (1998).
17. S. A. Chen and G. W. Hwang, *J. Am. Chem. Soc.*, **116**, 7939 (1994).
18. J. Roncali, *Chem. Rev. (Washington, D.C.)*, **92**, 711 (1992).
19. P. N. Bartlett and J. M. Cooper, *J. Electroanal. Chem.*, **362**, 1 (1993).
20. H. Ding and S.-M. Park, *J. Electrochem. Soc.*, **150**, E33 (2003).
21. J.-Y. Lee and S.-M. Park, *J. Electrochem. Soc.*, **147**, 4189 (2000).
22. Y. Yang and M. Wan, *J. Mater. Chem.*, **11**, 2022 (2001).
23. D. E. Stilwell and S.-M. Park, *J. Electrochem. Soc.*, **135**, 2254 (1988).
24. E. W. Paul, A. J. Ricco, and M. S. Wrighton, *J. Phys. Chem.*, **89**, 1441 (1985).
25. B.-S. Kim, W. H. Kim, and S. N. Hoier, and S.-M. Park, *Synth. Met.*, **69**, 455 (1995).
26. Y.-B. Shim and S.-M. Park, *J. Electrochem. Soc.*, **144**, 3027 (1997).
27. H. J. Lee, S.-Y. Cui, and S.-M. Park, *J. Electrochem. Soc.*, **148**, D139 (2001).
28. R. J. Waltman, A. F. Diaz, and J. Bargon, *J. Electrochem. Soc.*, **132**, 631 (1985).
29. J. Rault-Berthelot and J. Simonet, *J. Electroanal. Chem. Interfacial Electrochem.*, **182**, 187 (1985).
30. J. Rault-Berthelot and J. Simonet, *New J. Chem.*, **10**, 169 (1986).
31. J. Rault-Berthelot, L. Angely, J. Delaunay, and J. Simonet, *New J. Chem.*, **11**, 487 (1987).
32. J. Rault-Berthelot, V. Questaigne, and J. Simonet, *New J. Chem.*, **13**, 45 (1989).
33. J. Rault-Berthelot, G. Mabon, and J. Simonet, *J. Electroanal. Chem. Interfacial Electrochem.*, **240**, 355 (1988).
34. J. Rault-Berthelot, M. A. Orliak, and J. Simonet, *Electrochim. Acta*, **33**, 811 (1988).
35. J. Rault-Berthelot and M. M. Granger, *J. Electroanal. Chem.*, **353**, 341 (1993).
36. J. Simonet, J. Rault-Berthelot, M. M. Granger, and H. Le Diet, *J. Electroanal. Chem.*, **372**, 185 (1994).
37. J. Rault-Berthelot, M. Massaudi, H. Le Diet, and J. Simonet, *Synth. Met.*, **75**, 11 (1995).
38. J. Rault-Berthelot and M. M. Granger, *Synth. Met.*, **82**, 103 (1996).
39. D. Lorcy, J. Rault-Berthelot, and C. Poriel, *Electrochem. Commun.*, **2**, 382 (2000).
40. J.-I. Lee, D.-H. Hwang, H. Park, L.-M. Do, H. Y. Chu, T. Zyung, and R. D. Miller, *Synth. Met.*, **111-112**, 195 (2000).
41. M. Inbasekaran, E. Woo, W. Wu, M. Bernius, and L. Wujkowski, *Synth. Met.*, **111-112**, 397 (2000).
42. W. Porzio, C. Botta, S. Destri, and M. Pasini, *Synth. Met.*, **122**, 7 (2001).
43. A. Charas, J. Morgado, J. M. G. Martinho, L. Alcacer, S. F. Lim, R. H. Friend, and F. Cacialli, *Polymer*, **44**, 1843 (2003).
44. M. T. Bernius, M. Inbasekaran, J. O'Brien, and W. Wu, *Adv. Mater. (Weinheim, Ger.)*, **12**, 1737 (2000).
45. C. Carlin, L. J. Kepley, and A. J. Bard, *J. Electrochem. Soc.*, **132**, 353 (1985).
46. S. H. Glarum and J. H. Marshall, *J. Electrochem. Soc.*, **134**, 142 (1987).
47. S. J. Choi and S.-M. Park, *J. Electrochem. Soc.*, **149**, E26 (2002).
48. C.-H. Pyun and S.-M. Park, *Anal. Chem.*, **58**, 251 (1986).
49. (a) C. Zhang and S.-M. Park, *Anal. Chem.*, **60**, 1639 (1988); (b) C. Zhang and S.-M. Park, *Bull. Korean Chem. Soc.*, **10**, 302 (1989).
50. S.-y. Cui and S.-M. Park, *Synth. Met.*, **105**, 91 (1999).
51. (a) D. E. Stilwell and S.-M. Park, *J. Electrochem. Soc.*, **135**, 2491 (1988); (b) G. Tourillon, in *Handbook of Conducting Polymers*, T. A. Skotheim, Editor, Marcel Dekker, New York (1986).
52. *Physical Electrochemistry*, I. Rubinstein, Editor, Marcel Dekker, New York (1995).